

Grant agreement No: 101017008



# Harmony

Assistive robots for healthcare

## Enhancing Healthcare with Assistive Robotic Mobile Manipulation

(HARMONY) | H2020-ICT-2018-20 | RIA

Start of the project: 01.01.2021

Duration: 42 months

Deliverable Number	D7.3
Deliverable Name	Whole-body motion planning module for mobile manipulation
WP Number	7
Lead Beneficiary	UEDIN
Dissemination Level	Public
Internal Reviewer	CREATE
Due Date	29.12.2023
Date of Submission	
Version	0



This project has received funding from the European Union's Horizon 2020 research and innovation programme under grant agreement No 101017008

## Revision History

Version	Date	Author(s)	Comments
0	11/12/2023	Wenqian Du Joao Moura Jiayi Wang	First draft
1	11/12/2023	Mohammadreza Kasaei	draft
2	15/12/2023	Joao Moura	The final version for the internal review
3	29/12/2023	Fabio Ruggiero	Revised version

## Table of Contents

Revision History .....	2
Table of Contents .....	3
Summary.....	4
Introduction .....	5
Related publications .....	6
Planning and Whole-body Motion Generation Framework .....	6
Bezier Curve-based MPC.....	7
Bezier Curve based MPC for Compliance Control.....	9
Simulation and Experiments.....	10
Simulation Comparison with Traditional Discretized MPC.....	10
Experiment on Dynamic Obstacle Avoidance and Push Recovery .....	11
Conclusions.....	13
References.....	14

## Summary

The objective of this deliverable is to develop a whole-body motion planning module for mobile manipulation that can generate online robot motions, i.e., simultaneous motion of the mobile base and the dual arm system, which avoid workspace obstacles whilst being compliant in case of unexpected collisions and/or intended interactions by a human co-sharing the workspace. The mobile manipulator needs to react to unexpected situations which may happen in an anthropic environment and to ensure compliant behaviour of the robot to the external environment.

In summary, we successfully developed a Trajectory Optimization (TO) framework that splits the task and whole-body motion generation in two components that by using an efficient trajectory parameterization, based on Bezier curves, is able to generate task and robot configuration motions online in a Model Predictive Control (MPC) fashion, which enables the robot to adapt its motions to a dynamic environment, for instance to moving obstacles, and to comply and react to unplanned physical interactions.

## Introduction

The challenges tackled by Harmony, specifically the use case 2 illustrated in Figure 1, require the motion generation and execution of dexterous coordinated tasks between the mobile base and the robot manipulators. State-of-the-art manipulation planning techniques fall short in terms of safety and robustness, especially in fast-changing uncontrolled environments, such as the hospital floor. The goal of this deliverable within WP7 (D7.3) is to enable the mobile manipulator to react to unexpected situations, which may happen in an anthropic environment, while replanning the target task.

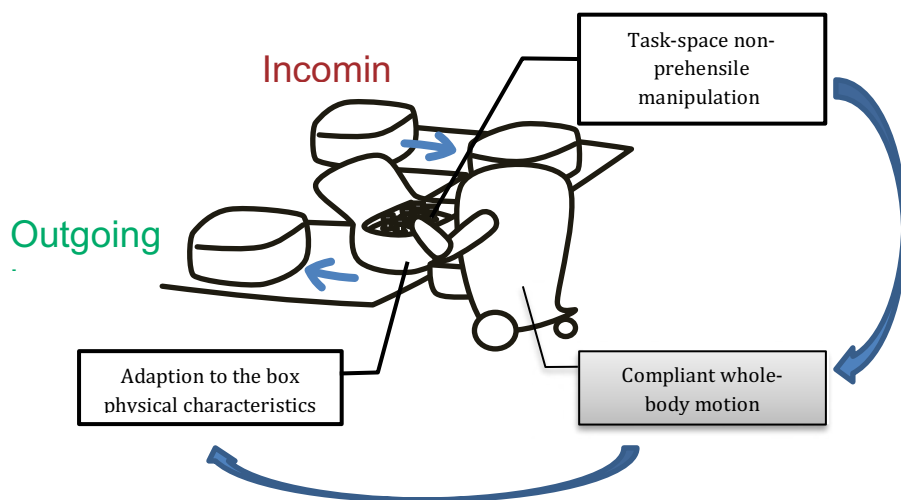


Figure 1. Diagram of bioassay flow automation use case.

Dual-arm mobile manipulation can enable handling large-size objects by grasping and carrying. However, dynamically changing environments require online planning of the motion and whole-body compliant behaviours. Current state-of-the-art methods are incapable of online planning and tracking of mobile manipulator motions in a receding horizon and, therefore, lack reliability on compliant interaction. We propose a novel predictive whole-body motion generator for high degree-of-freedom (DOF) dual-arm position/velocity-controlled mobile manipulators. To the best of our knowledge, we are the first to integrate Bezier-curve parameterization for whole-body joint-trajectory optimization and admittance control using a Model-based Predictive Control (MPC) framework. Consequently, this setting equips MPC with continuous properties and fewer optimization variables. It also strengthens the highly redundant mobile manipulator to predict long-horizon end-effector trajectory and whole-body compliant motion and interact efficiently with subjects and the environment in real-time. The simulated and real-world experiments demonstrate the robustness and effectiveness of this framework.

In summary, we have achieved the following functionalities and performance:

- We propose an efficient parameterization of the Trajectory Optimization to speedup MPC computation through Bezier curve transcription.
- We propose an MPC framework that decomposes the real-time motion generation into an end-effector task-space motion planning for long horizons, and whole-body motion planning in a relatively long horizon, which integrates admittance control.
- We conduct several simulations and experiment comparisons between a standard MPC method, and our Bezier curve based MPC, which show the effectiveness of our framework.

## Related publications

“An Efficient Representation of Model Predictive Control for Compliant Dual-arm Mobile Manipulation”, Wenqian Du, Ran Long, Joao Moura, Jiayi Wang, Saeid Samadi, Sethu Vijayakumar, under review, IEEE Transactions on Robotics.

## Planning and Whole-body Motion Generation Framework

We apply a two-stage MPC framework, shown in Figure 2 to enable the real-time planning and whole-body motion generation. The control framework contains a trajectory planner and a tracking controller. The former one concentrates on the motion planning for dual-arm end-effectors, and the latter one focuses on the local-motion tracking.

By given the object target, the first MPC is built in the task space to achieve the optimal end-effector trajectory  $h(t)$  for long horizon, while including collision avoidance constraint to ensure safe distance. The cost function is to minimize the end-effector trajectory distance, velocity and acceleration that satisfy the initial and target states. This MPC should run at high frequencies to react to dynamic obstacles.

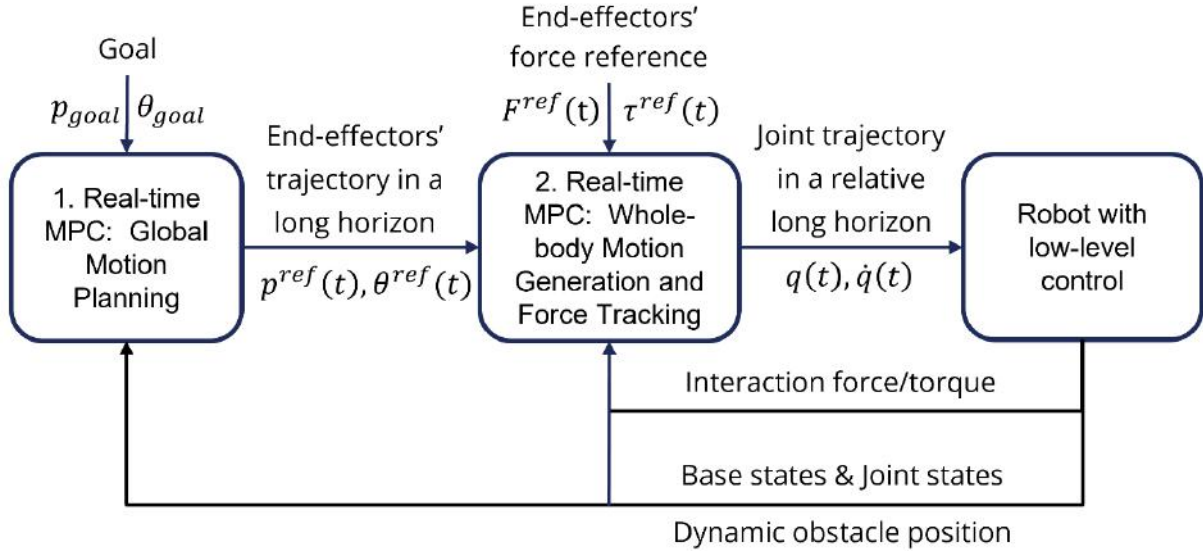


Figure 2. Two-stage framework of whole-body compliant motion generation using model-based predictive control.

The second part of our framework consists of a second MPC built in joint space to track the planned end-effector trajectory and a given force/torque trajectory reference. Admission controller is integrated in this MPC to achieve efficient force/torque tracking. This MPC optimizes the whole-body joint position, velocity, and end-effector force/torque trajectories in a relatively long horizon. This MPC also includes collision avoidance constraints, between the end-effectors/mobile base and the dynamic obstacle. Despite this two-stage MPC framework, with traditional direct collocation discretization fail to accomplish a sufficiently low computation time that would lead to a high enough frequency controller required for this type of tasks, especially for the whole-body MPC case. In this section, we solve this issue by proposing a new approach via reducing the number of decision variables to speed up the two-stage MPCs.

## Bezier Curve-based MPC

In dynamically changing environments, we expect to be able to execute the task and whole-body MPCs at high frequencies, e.g., higher than 50 Hz. Including strict constraints, such as safety conditions, in the trajectory optimization makes it difficult to solve it fast. Therefore, we propose an efficient representation in this section. Consider a generic time parameterized trajectory  $\varepsilon(t)$ , we can formulate the trajectory optimization problem as follows,

$$\begin{aligned} \min_{\varepsilon(t)} \int_0^T L(\varepsilon(t)) \\ s.t. \quad g(\varepsilon(t)) \leq 0, \forall t \in [0, T] \end{aligned}$$

where  $L()$  is the lost function.  $g()$  is the constraint function. In general, there is no solution for this infinite dimensional problem. One way of solving is through direct collocation that discretizes the trajectory in sampling time knots. The most typical approach is to have equidistant sampling points and approximate the equations of motion by linear or trapezoidal local approximations. Then the trajectory optimization problem, shown in Figure 3(b), is formulated as below,

$$\min_{\varepsilon_{[0, \dots, K]}} \sum_0^K L(\varepsilon_i)$$

$$s. t. \quad g(\varepsilon_i) \leq 0, \forall i \in [0, \dots, k]$$

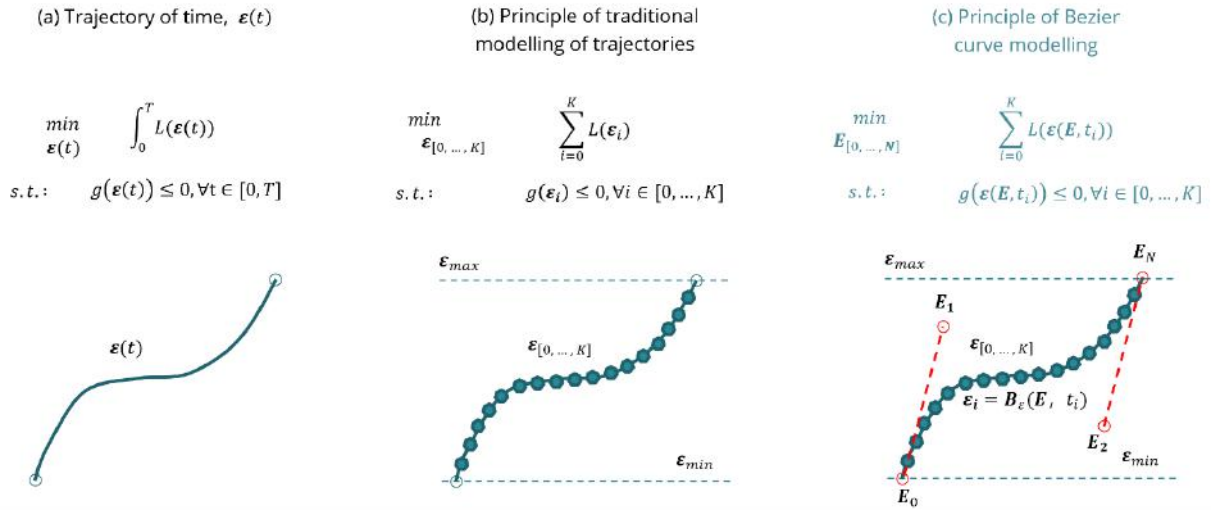


Figure 3. (a) Robot state trajectory as function of time; (b) Discretized robot states at sampling time knots; (c) Representation of the Bezier-curve transcription.

where  $\varepsilon_i$  is the state at  $i$ 's time knot. However, it requires dense sampling time knots when it needs good planning/tracking performance, resulting in many decision variables. In addition, at each time knot, its position, velocity, and acceleration can also be decision variables which further increases the number of decision variables. Therefore, the traditional discretization approach slows down the computation. In this work, we propose an efficient representation of trajectories, which enables fast computation with off-the-shell solvers.

We transcript kinds of trajectories relating to the whole-body motion as Bezier curves to reduce the number of decision variables. A Bezier curve is parameterized by its control points which constitute the convex hull of the whole curve [1]. Then few control points of the Bezier curve can be applied as the decision variable. At each time knot, the robot state is the function of the control points. The trajectories in the planner and MPC-based controller can be defined in the task space or joint space. In general, it is defined as follows,

$$\varepsilon(t) = B_{\varepsilon}(E, \bar{t}),$$



where  $E = [E_0 \cdots E_K] \in \mathbb{R}^{n_\varepsilon \times K}$  denotes the control points on the Bezier curve, and  $n_\varepsilon$  denotes the DOF that the state  $\varepsilon$  accounts for  $\bar{t} = \frac{t-t_0}{T}$  is the normalized time,  $0 \leq \bar{t} \leq 1$ ,  $t$  is the real time and  $t_0$  is the starting time of each control loop.  $T$  is the horizon and is equal to be 1s and  $K$  is defined to be 10.  $E_0$  and  $E_K$  denote the beginning ( $t = 0$ ) and end ( $t = 1$ ) state configuration. The differential of a Bezier curve is also a Bezier curve, using the same set of control points, this property enables us to constrain the state velocities and accelerations in a straight manner.

This setting embodies the following advantages:

- No need for model transition among sampling states, because the robot model in different order can be expressed analytically, such as the whole-body dynamics model using the same set of control points for joint position, velocity, and acceleration. For example, no need to differentialize model states approximately since analytical expressions are available.
- With continuous property, the number of discretized time knots  $K$  can be reduced, further reducing the number of decision variable compared to classical MPC, e.g., a straight line needs only two control points.
- Admittance control can also borrow strengths of Bezier-curve parametrization to generate motion in position/orientation level instead of noisy velocities and enable better tracking performance of the interaction force/torque.
- Constraining the control points directly within a limit range  $\varepsilon_{min} \leq E_i \leq \varepsilon_{max}$ ,  $i \in [0, \dots, K]$  enables that the whole curve will satisfy the limit range in Figure 3(c).
- Real-time calculation which enables mobile manipulators to behave more efficiently in changing environments.

This efficient representation enables fast calculation of the planning and whole-body tracking MPCs.

## Bezier Curve based MPC for Compliance Control

Since our dual-arm mobile manipulator is position and velocity controlled, force/torque sensors are only available at two end-effectors, and admittance control can be applied to enable compliance at two end-effectors' operational space, by transferring force/torque deviation to end-effector motions. For conventional admittance control, by given the desired and actual force/torque, only the end-effector velocities can be achieved. In this work, the Bezier curve-based parametrization is applied and integrated in admittance control, and further enables the generation of end-effector positions and accelerations.

Therefore, the force tracking controller can be defined simply as an additional equality constraint in the end-effector motion generation,

$$F^{ref}(t) = F_{actual}^{ext} + \Lambda_p \ddot{\tilde{p}}(t) + K_p \tilde{p}(t) + D_p \dot{\tilde{p}}(t),$$

where  $F_{actual}^{ext}$  is the actual interaction force at the beginning of each control loop. By given the interaction force reference relating to time  $F^{ref}(t)$ , the optimization of  $\tilde{p}(t)$  can be added into the MPC framework. Traditional MPC based impedance controllers treat the  $\tilde{p}(t)$ ,  $\dot{\tilde{p}}(t)$ , and  $\ddot{\tilde{p}}(t)$  as different optimization variables [3] [4] [5]. With the Bezier curve parameterization,  $\tilde{p}(t)$  can also be built as a Bezier curve as follows:

$$\tilde{p}(t) = B_{\tilde{p}}(\tilde{P}, \tilde{t}).$$

## Simulation and Experiments

In the simulation and experiment, the dual-arm mobile manipulator picks up a box on a desk and carries it to another desk, meanwhile, avoids an obstacle. The whole process is divided into 5 phases. The ground truth is built by using Vicon cameras which are also applied to get poses of the robot mobile base and a box. We apply OpTaS [6], a task specification Python library to build our motion planner and MPC controller that builds on top of CasADI [7] and use KNITRO as the nonlinear problem solver [2]. By detecting the box pose, the motion planner optimizes and updates the trajectory online in each phase. The controllers track this trajectory and conducts admittance-based compliance control when two end-effectors interact with the box. The calculations are executed on a workstation with an Intel i9 3.6GHz CPU, and the outputs are sent to the robot by wireless router. The two MPCs for task-space and whole-body motion generation run in series, and the full process runs at 50Hz.

### Simulation Comparison with Traditional Discretized MPC

We compare the tracking performance of the standard transcription without Bezier-curve representation, as shown in Figure 4(a) on the solver time, Figure 4(b) on the tracking performance, and the comparison result, as shown in Tab. 1. By given a “S”-shape position references for two end-effectors, the two MPCs generate whole-body motion to track the pre-defined task-space motion references (without force tracking in this part). We can see that for traditional whole-body MPC, when the time knot number is small, the tracking error is relatively high. To improve the tracking performance, the calculation time of traditional MPC becomes very slow. We can see that with the same long horizon and time knots, our Bezier-curve based whole-body MPC runs faster and with better tracking performance. Since our method reduces the decision variable number, for dense time knots, our method still runs quite fast with satisfactory tracking performance.

Table 1. Comparison between traditional MPC and our Bezier curve based MPC.

Items	MPC (Traditional)		MPC (Bézier curve)	
Long horizon	5s	5s	5s	5s
Time knots	$K = 6$	$K = 26$	$K = 6$	$K = 26$
Control point No.	-	-	$N_q = 6$	$N_q = 6$
Decision variable	$\mathbf{q}_{[0 \dots K]}$ and $\dot{\mathbf{q}}_{[0 \dots K]}$	$\mathbf{q}_{[0 \dots K]}$ and $\dot{\mathbf{q}}_{[0 \dots K]}$	$\mathbf{Q}_{[0 \dots N_q]}$	$\mathbf{Q}_{[0 \dots N_q]}$
Decision variable No.	$2K \times n_{dof} = 216$	$2K \times n_{dof} = 936$	$N \times n_{dof} = 108$	$N \times n_{dof} = 108$
Average computation time	11ms	58ms	9ms	12ms
Max tracking error	19.4cm	9.8cm	7.8cm	5.4cm

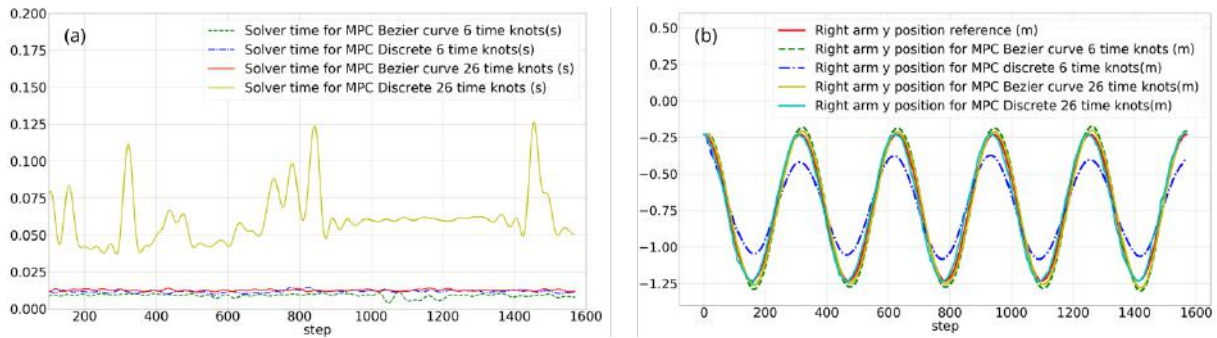


Figure 4. (a) Solving time of standard MPC and our Bezier curve based MPC. (b) Tracking performance of standard MPC and our Bezier curve based MPC.

## Experiment on Whole-body Motion Generation for Static Obstacle Avoidance

In this scenario, we test the whole-body motion generation for static obstacle avoidance, shown in Figure 5. EVA transports a box from the left table to the right table. In the middle of two tables, an obstacle is placed which enforces EVA to lift the two arms automatically. There is another obstacle near the right table which is used to enforce EVA to twist its mobile base while placing the box.

## Experiment on Navigation in Narrow Spaces

In this scenario, we evaluate our method in a more complex environment, shown in Fig 6. The robot transports a box and pass a narrow space. As motion planning only accounts for the obstacle avoidance between end-effectors and the narrow walls which are not wide enough for EVA to traverse sideways, then the whole-body MPC will enforce the whole robot to turn before passing the narrow path based on the obstacle avoidance between the mobile base and the walls.

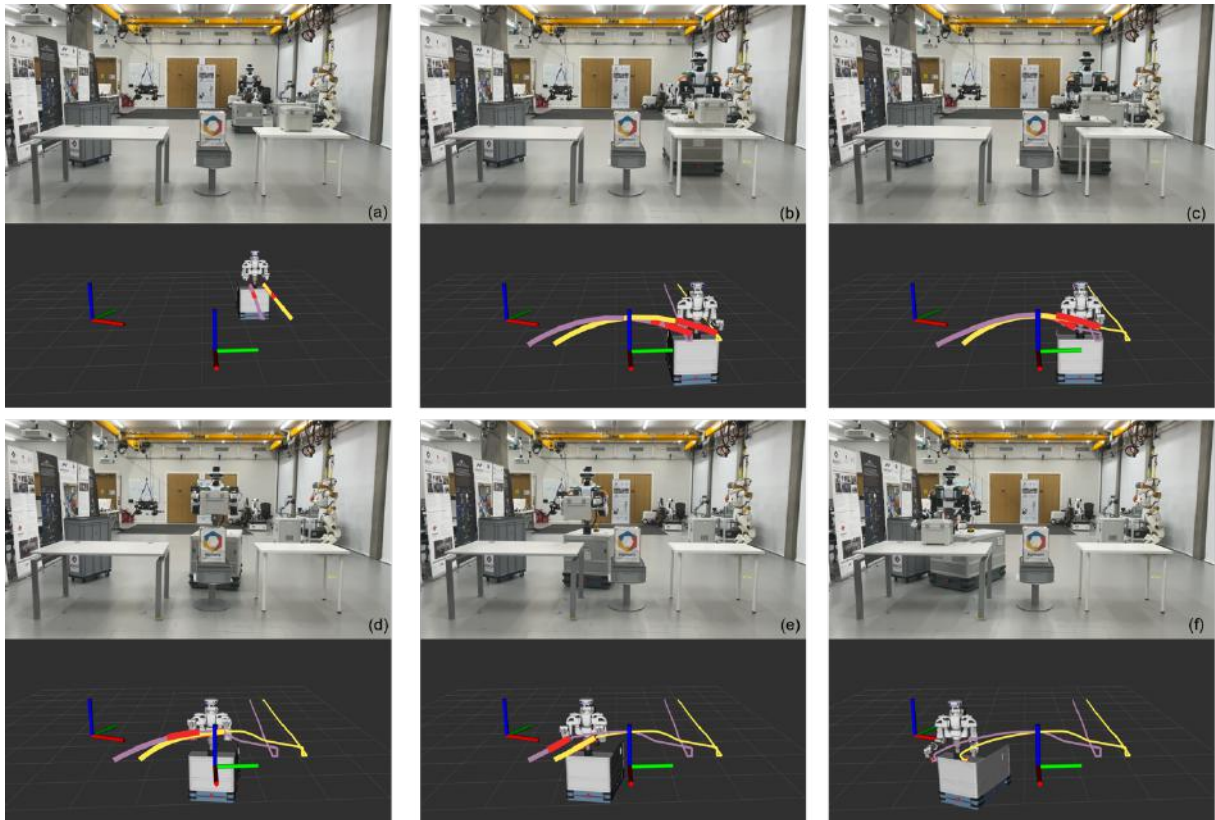


Figure 5. Whole-body motion while avoiding static obstacles.

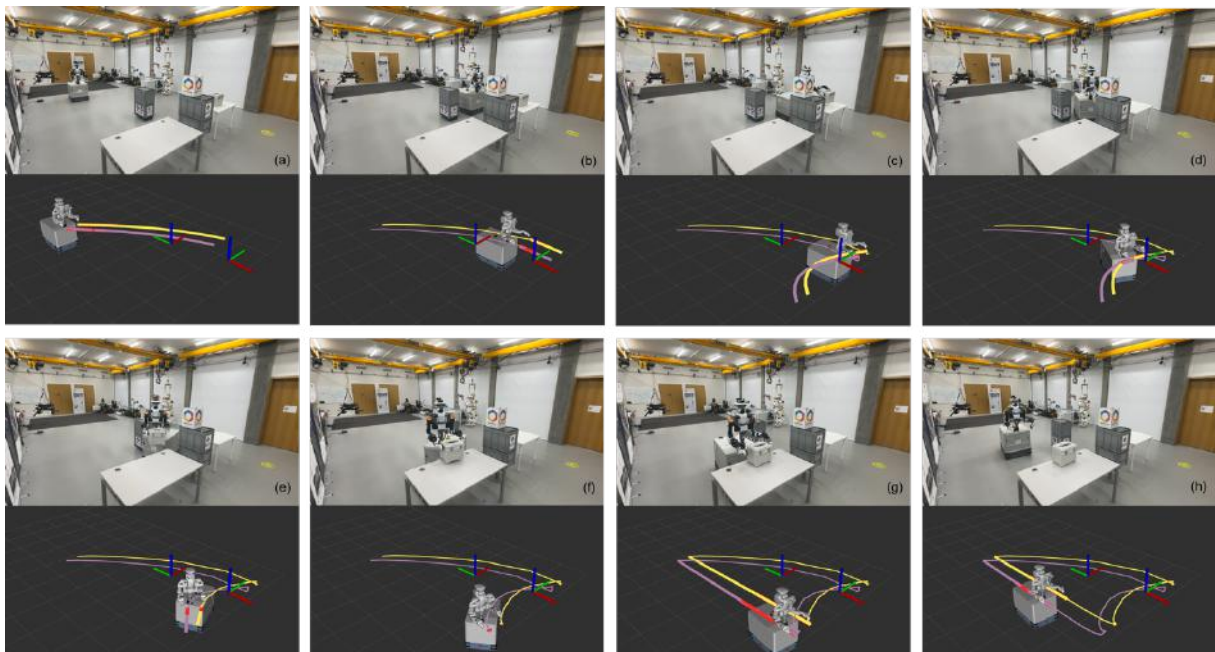


Figure 6. Whole-body motion in narrow spaces.

## Experiment on Dynamic Obstacle Avoidance and Push Recovery

In this scenario, we show the capabilities of dynamic interaction with external disturbances, including dynamic obstacle avoidance and push recovery. When EVA (the mobile robot in Figure 7 transports the box, we push an obstacle to approach the robot. The robot re-plans and generates whole-body motion online, and avoids the dynamic obstacle with a smooth path, as shown in Figure 7. When the robot is near the table, we push the robot hand and the whole-body MPC generates compliant motion. After the push, the robot recovers and manages the remaining of the task.

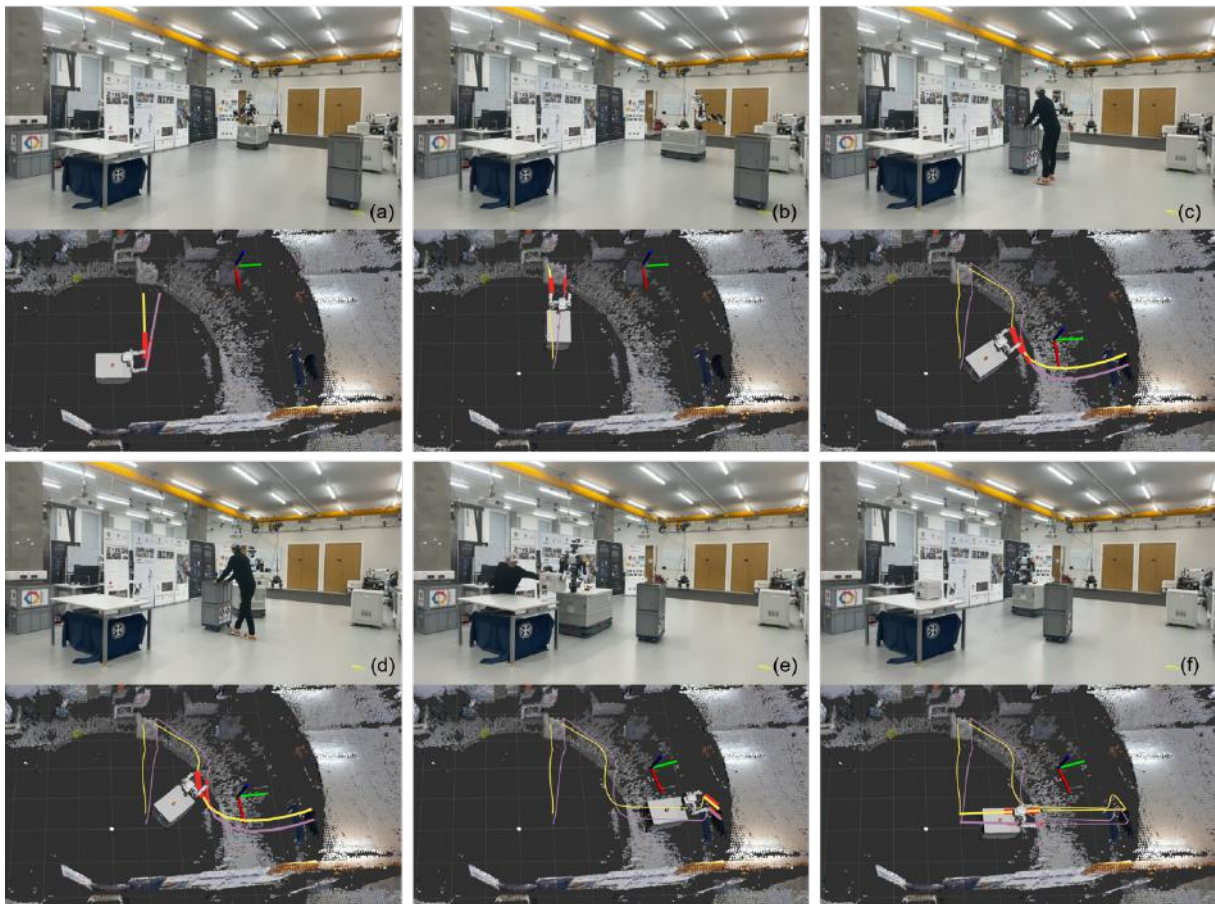


Figure 7. Whole-body motion while performing dynamic obstacle avoidance and compliant push-recovery motion.

## Conclusions

This work integrates Bezier-curve parameterization into a two-stage MPC framework which reduces the decision variable number dramatically. With hard constraints, our method shows strengths on real-time calculation and tracking performance using whole-body motion for highly redundant dual-arm mobile manipulation. The concept of efficient representation of whole-body trajectory optimization enables the motion planning in a long horizon, compliant

whole-body motion generation in a relative long horizon be executed in real time. The two-stage MPCs enable the robot to behave compliantly to external disturbances while avoiding dynamic obstacles.

## References

- [1] P. Fernbach, S. Tonneau, O. Stasse, J. Carpentier, and M. Taix, “C-croc: Continuous and convex resolution of centroidal dynamic trajectories for legged robots in multicontact scenarios,” *IEEE Transactions on Robotics*, vol. 36, no. 3, pp. 676–691, 2020.
- [2] R. H. Byrd, J. Nocedal, and R. A. Waltz, “Knitro: An integrated package for nonlinear optimization,” *Large-scale nonlinear optimization*, pp. 35–59, 2006.
- [3] M. Bednarczyk, H. Omran, and B. Bayle, “Model predictive impedance control,” in *2020 IEEE international conference on robotics and automation (ICRA)*, 2020.
- [4] Z. Jin, D. Qin, A. Liu, W.-a. Zhang, and L. Yu, “Model predictive variable impedance control of manipulators for adaptive precision- compliance trade off,” *IEEE/ASME Transactions on Mechatronics*, vol. 28, no. 2, pp. 1174–1186, 2022.
- [5] T. Gold, A. Voßl, and K. Graichen, “Model predictive interaction control for robotic manipulation tasks,” *IEEE Transactions on Robotics*, vol. 39, no. 1, pp. 76–89, 2022.
- [6] C. E. Mower, J. Moura, N. Z. Behabadi, S. Vijayakumar, T. Vercauteren, and C. Bergeles, “Optas: An optimization-based task specification library for trajectory optimization and model predictive control,” *IEEE international conference on robotics and automation (ICRA)*, 2022.
- [7] J. A. E. Andersson, J. Gillis, G. Horn, J. B. Rawlings, and M. Diehl, “CasADi – A software framework for nonlinear optimization and optimal control,” *Mathematical Programming Computation*, vol. 11, no. 1, pp. 1–36, 2019.